

Quarkonium inclusive production: negative NLO cross sections, scale fixing and high-energy resummation

J.P. Lansberg

IJCLab Orsay – Paris-Saclay U. – CNRS

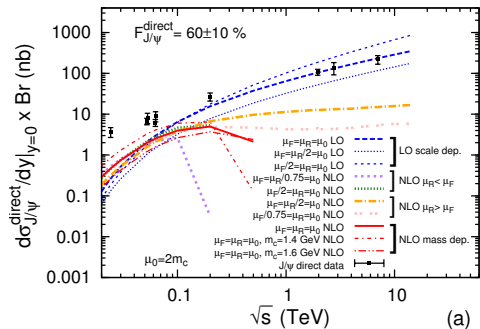
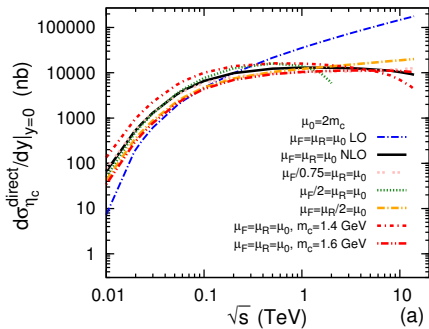
Diffraction and Low- x 2022

24-30 Sept 2022 Corigliano Calabro, Italy



This project is supported by the European Union's Horizon 2020 research and innovation programme under Grant agreement no. 824093

Problem of negative cross sections - η_c and J/ψ at NLO



(N)LO η_c (left) and J/ψ (right) cross sections vs \sqrt{s} for different scale choices of μ_R and μ_F with CTEQ6M

[Y. Feng, JPL, J.X. Wang, Eur.Phys.J. C75 (2015) 313]

η_c at NLO - historical developments

- J. Kühn & E. Mirkes compute pseudo-scalar toponium cross section at NLO in 1992

[J. Kühn, E. Mirkes, Phys.Lett. B296 (1992) 425-429]

η_c at NLO - historical developments

- J. Kühn & E. Mirkes compute pseudo-scalar toponium cross section at NLO in 1992
[J. Kühn, E. Mirkes, Phys.Lett. B296 (1992) 425-429]
- G. Schuler's review in 1994
[G. Schuler, arXiv:hep-ph/9403387]

η_c at NLO - historical developments

- J. Kühn & E. Mirkes compute pseudo-scalar toponium cross section at NLO in 1992
[J. Kühn, E. Mirkes, Phys.Lett. B296 (1992) 425-429]
- G. Schuler's review in 1994
• confirms result by J. Kühn & E. Mirkes
[G. Schuler, arXiv:hep-ph/9403387]

η_c at NLO - historical developments

- J. Kühn & E. Mirkes compute pseudo-scalar toponium cross section at NLO in 1992
[J. Kühn, E. Mirkes, Phys.Lett. B296 (1992) 425-429]
- G. Schuler's review in 1994
[G. Schuler, arXiv:hep-ph/9403387]
 - confirms result by J. Kühn & E. Mirkes
 - points out issues with negative cross sections at high energies

η_c at NLO - historical developments

- J. Kühn & E. Mirkes compute pseudo-scalar toponium cross section at NLO in 1992
[J. Kühn, E. Mirkes, Phys.Lett. B296 (1992) 425-429]
- G. Schuler's review in 1994
 - confirms result by J. Kühn & E. Mirkes
 - points out issues with negative cross sections at high energies
 - explains why, for some gluon PDF shapes, appearance of strong/weak μ_F dependence[G. Schuler, arXiv:hep-ph/9403387]

η_c at NLO - historical developments

- J. Kühn & E. Mirkes compute pseudo-scalar toponium cross section at NLO in 1992
[J. Kühn, E. Mirkes, Phys.Lett. B296 (1992) 425-429]
- G. Schuler's review in 1994
[G. Schuler, arXiv:hep-ph/9403387]
 - confirms result by J. Kühn & E. Mirkes
 - points out issues with negative cross sections at high energies
 - explains why, for some gluon PDF shapes, appearance of strong/weak μ_F dependence
- M. Mangano comes to same conclusions as G. Schuler in his 1997 Proceedings
[M.L. Mangano, A. Petrelli, Int.J.Mod.Phys. A12 (1997) 3887-3897]

η_c at NLO - historical developments

- J. Kühn & E. Mirkes compute pseudo-scalar toponium cross section at NLO in 1992
[J. Kühn, E. Mirkes, Phys.Lett. B296 (1992) 425-429]
- G. Schuler's review in 1994
[G. Schuler, arXiv:hep-ph/9403387]
 - confirms result by J. Kühn & E. Mirkes
 - points out issues with negative cross sections at high energies
 - explains why, for some gluon PDF shapes, appearance of strong/weak μ_F dependence
- M. Mangano comes to same conclusions as G. Schuler in his 1997 Proceedings
[M.L. Mangano, A. Petrelli, Int.J.Mod.Phys. A12 (1997) 3887-3897]
- A. Petrelli *et al.* confirm result by J. Kühn & E. Mirkes in 1998
[A. Petrelli et al., Nucl.Phys. B514 (1998) 245-309]

η_c at NLO - historical developments

- J. Kühn & E. Mirkes compute pseudo-scalar toponium cross section at NLO in 1992
[J. Kühn, E. Mirkes, Phys.Lett. B296 (1992) 425-429]
- G. Schuler's review in 1994
[G. Schuler, arXiv:hep-ph/9403387]
 - confirms result by J. Kühn & E. Mirkes
 - points out issues with negative cross sections at high energies
 - explains why, for some gluon PDF shapes, appearance of strong/weak μ_F dependence
- M. Mangano comes to same conclusions as G. Schuler in his 1997 Proceedings
[M.L. Mangano, A. Petrelli, Int.J.Mod.Phys. A12 (1997) 3887-3897]
- A. Petrelli *et al.* confirm result by J. Kühn & E. Mirkes in 1998
[A. Petrelli et al., Nucl.Phys. B514 (1998) 245-309]
- We reached the same conclusions
[M.A. Ozcelik, PoS DIS2019 (2019) 159, Y. Feng, JPL, J.X. Wang, Eur.Phys.J. C75 (2015) 313]

η_c at NLO - historical developments

- J. Kühn & E. Mirkes compute pseudo-scalar toponium cross section at NLO in 1992
[J. Kühn, E. Mirkes, Phys.Lett. B296 (1992) 425-429]
- G. Schuler's review in 1994
[G. Schuler, arXiv:hep-ph/9403387]
 - confirms result by J. Kühn & E. Mirkes
 - points out issues with negative cross sections at high energies
 - explains why, for some gluon PDF shapes, appearance of strong/weak μ_F dependence
- M. Mangano comes to same conclusions as G. Schuler in his 1997 Proceedings
[M.L. Mangano, A. Petrelli, Int.J.Mod.Phys. A12 (1997) 3887-3897]
- A. Petrelli *et al.* confirm result by J. Kühn & E. Mirkes in 1998
[A. Petrelli et al., Nucl.Phys. B514 (1998) 245-309]
- We reached the same conclusions
[M.A. Ozcelik, PoS DIS2019 (2019) 159, Y. Feng, JPL, J.X. Wang, Eur.Phys.J. C75 (2015) 313]
- For a recent review on quarkonium-production mechanisms in general
[J.-P. Lansberg, Phys.Rept. 889 (2020) 1]

The NLO partonic cross section at large \hat{s}

The **partonic high-energy limit** is defined as taking $\hat{\sigma}$ at $\hat{s} \rightarrow \infty$ or equivalently $z \rightarrow 0$ with $z = \frac{M_Q^2}{\hat{s}}$,

$$\lim_{z \rightarrow 0} \hat{\sigma}_{gg}^{\text{NLO}}(z) = 2C_A \frac{\alpha_s}{\pi} \hat{\sigma}_0^{\text{LO}} \left(\log \frac{M_Q^2}{\mu_F^2} + A_{gg} \right) \quad (1)$$

$$\lim_{z \rightarrow 0} \hat{\sigma}_{qg}^{\text{NLO}}(z) = C_F \frac{\alpha_s}{\pi} \hat{\sigma}_0^{\text{LO}} \left(\log \frac{M_Q^2}{\mu_F^2} + A_{qg} \right) \quad (2)$$

The NLO partonic cross section at large \hat{s}

The **partonic high-energy limit** is defined as taking $\hat{\sigma}$ at $\hat{s} \rightarrow \infty$ or equivalently $z \rightarrow 0$ with $z = \frac{M_Q^2}{\hat{s}}$,

$$\lim_{z \rightarrow 0} \hat{\sigma}_{gg}^{\text{NLO}}(z) = 2C_A \frac{\alpha_s}{\pi} \hat{\sigma}_0^{\text{LO}} \left(\log \frac{M_Q^2}{\mu_F^2} + A_{gg} \right) \quad (1)$$

$$\lim_{z \rightarrow 0} \hat{\sigma}_{qg}^{\text{NLO}}(z) = C_F \frac{\alpha_s}{\pi} \hat{\sigma}_0^{\text{LO}} \left(\log \frac{M_Q^2}{\mu_F^2} + A_{qg} \right) \quad (2)$$

- for ${}^1S_0^{[1,8]}$:

$$A_{gg} = A_{qg} = -1$$

The NLO partonic cross section at large \hat{s}

The **partonic high-energy limit** is defined as taking $\hat{\sigma}$ at $\hat{s} \rightarrow \infty$ or equivalently $z \rightarrow 0$ with $z = \frac{M_Q^2}{\hat{s}}$,

$$\lim_{z \rightarrow 0} \hat{\sigma}_{gg}^{\text{NLO}}(z) = 2C_A \frac{\alpha_s}{\pi} \hat{\sigma}_0^{\text{LO}} \left(\log \frac{M_Q^2}{\mu_F^2} + A_{gg} \right) \quad (1)$$

$$\lim_{z \rightarrow 0} \hat{\sigma}_{qg}^{\text{NLO}}(z) = C_F \frac{\alpha_s}{\pi} \hat{\sigma}_0^{\text{LO}} \left(\log \frac{M_Q^2}{\mu_F^2} + A_{qg} \right) \quad (2)$$

- for ${}^1S_0^{[1,8]}$: $A_{gg} = A_{qg} = -1$
- for $\mu_F = M_Q$, $\hat{\sigma}_{ig}^{\text{NLO}}(\hat{s} \rightarrow \infty) \propto -\frac{\alpha_s}{\pi} \hat{\sigma}_0^{\text{LO}}$

The NLO partonic cross section at large \hat{s}

The **partonic high-energy limit** is defined as taking $\hat{\sigma}$ at $\hat{s} \rightarrow \infty$ or equivalently $z \rightarrow 0$ with $z = \frac{M_Q^2}{\hat{s}}$,

$$\lim_{z \rightarrow 0} \hat{\sigma}_{gg}^{\text{NLO}}(z) = 2C_A \frac{\alpha_s}{\pi} \hat{\sigma}_0^{\text{LO}} \left(\log \frac{M_Q^2}{\mu_F^2} + A_{gg} \right) \quad (1)$$

$$\lim_{z \rightarrow 0} \hat{\sigma}_{qg}^{\text{NLO}}(z) = C_F \frac{\alpha_s}{\pi} \hat{\sigma}_0^{\text{LO}} \left(\log \frac{M_Q^2}{\mu_F^2} + A_{qg} \right) \quad (2)$$

- for ${}^1S_0^{[1,8]}$: $A_{gg} = A_{qg} = -1$
- for $\mu_F = M_Q$, $\hat{\sigma}_{ig}^{\text{NLO}}(\hat{s} \rightarrow \infty) \propto -\frac{\alpha_s}{\pi} \hat{\sigma}_0^{\text{LO}}$
- this limit contributes most for “flat” gluon PDFs at low x

The NLO partonic cross section at large \hat{s}

The **partonic high-energy limit** is defined as taking $\hat{\sigma}$ at $\hat{s} \rightarrow \infty$ or equivalently $z \rightarrow 0$ with $z = \frac{M_Q^2}{\hat{s}}$,

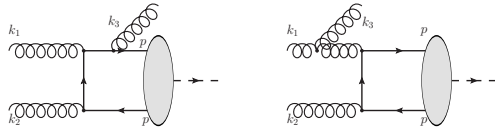
$$\lim_{z \rightarrow 0} \hat{\sigma}_{gg}^{\text{NLO}}(z) = 2C_A \frac{\alpha_s}{\pi} \hat{\sigma}_0^{\text{LO}} \left(\log \frac{M_Q^2}{\mu_F^2} + A_{gg} \right) \quad (1)$$

$$\lim_{z \rightarrow 0} \hat{\sigma}_{qg}^{\text{NLO}}(z) = C_F \frac{\alpha_s}{\pi} \hat{\sigma}_0^{\text{LO}} \left(\log \frac{M_Q^2}{\mu_F^2} + A_{qg} \right) \quad (2)$$

- for ${}^1S_0^{[1,8]}$: $A_{gg} = A_{qg} = -1$
- for $\mu_F = M_Q$, $\hat{\sigma}_{ig}^{\text{NLO}}(\hat{s} \rightarrow \infty) \propto -\frac{\alpha_s}{\pi} \hat{\sigma}_0^{\text{LO}}$
- this limit contributes most for “flat” gluon PDFs at low x
- If PDFs are not steep (evolved) enough, the large- \hat{s} region dominates and the hadronic cross section becomes negative

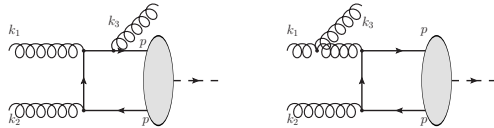
Recap of NLO calculation & origin of negative numbers

\hat{s} -dependence only present in real corrections ($g(k_1) + g(k_2) \rightarrow \eta_Q(P) + g(k_3)$)



Recap of NLO calculation & origin of negative numbers

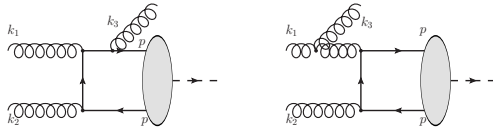
\hat{s} -dependence only present in real corrections ($g(k_1) + g(k_2) \rightarrow \eta_Q(P) + g(k_3)$)



- Real-emission corrections are perfect square ($|\mathcal{M}^{(\text{Real})}|^2$) and thus positive

Recap of NLO calculation & origin of negative numbers

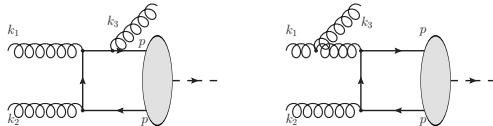
\hat{s} -dependence only present in real corrections ($g(k_1) + g(k_2) \rightarrow \eta_Q(P) + g(k_3)$)



- Real-emission corrections are perfect square ($|\mathcal{M}^{(\text{Real})}|^2$) and thus positive
- IR singularities in the real emissions only reveal themselves after taking the phase-space integration: $\bar{\sigma}_{gg}^{\text{NLO}, z \neq 1}(z) = \int d\hat{t} \frac{\bar{\sigma}_{gg}^{\text{NLO}, z \neq 1}}{d\hat{t}}$

Recap of NLO calculation & origin of negative numbers

\hat{s} -dependence only present in real corrections ($g(k_1) + g(k_2) \rightarrow \eta_Q(P) + g(k_3)$)



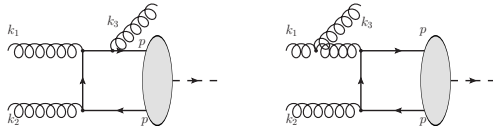
- Real-emission corrections are perfect square ($|\mathcal{M}^{(\text{Real})}|^2$) and thus positive
- IR singularities in the real emissions only reveal themselves after taking the

$$\text{phase-space integration: } \overline{\sigma}_{gg}^{\text{NLO}, z \neq 1}(z) = \int d\hat{t} \frac{\overline{\sigma}_{gg}^{\text{NLO}, z \neq 1}}{d\hat{t}}$$

$$\overline{\sigma}_{gg}^{\text{NLO}, z \neq 1}(z) = -\frac{1}{\epsilon_{\text{IR}}} \frac{\alpha_s}{\pi} \left(\frac{4\pi\mu_R^2}{M_Q^2} \right)^\epsilon \Gamma(1+\epsilon) \hat{\sigma}_0^{\text{LO}} z P_{gg}(z) + 2C_A \frac{\alpha_s}{\pi} \hat{\sigma}_0^{\text{LO}} \overline{A}_{gg}(z)$$

Recap of NLO calculation & origin of negative numbers

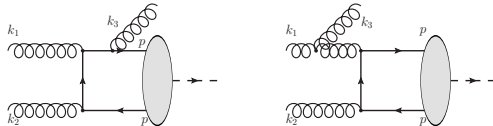
\hat{s} -dependence only present in real corrections ($g(k_1) + g(k_2) \rightarrow \eta_Q(P) + g(k_3)$)



- Real-emission corrections are perfect square ($|\mathcal{M}^{(\text{Real})}|^2$) and thus **positive**
- IR singularities in the real emissions only reveal themselves after taking the phase-space integration: $\overline{\sigma}_{gg}^{\text{NLO}, z \neq 1}(z) = \int d\hat{t} \frac{\overline{\sigma}_{gg}^{\text{NLO}, z \neq 1}}{d\hat{t}}$
$$\overline{\sigma}_{gg}^{\text{NLO}, z \neq 1}(z) = -\frac{1}{\epsilon_{\text{IR}}} \frac{\alpha_s}{\pi} \left(\frac{4\pi\mu_R^2}{M_Q^2} \right)^\epsilon \Gamma(1+\epsilon) \hat{\sigma}_0^{\text{LO}} z P_{gg}(z) + 2C_A \frac{\alpha_s}{\pi} \hat{\sigma}_0^{\text{LO}} \overline{A}_{gg}(z)$$
- For $\epsilon_{\text{IR}} \rightarrow 0^-$, $\overline{\sigma}_{gg}^{\text{NLO}, z \neq 1} \geq 0$ for all $0 \leq z < 1$ as expected

Recap of NLO calculation & origin of negative numbers

\hat{s} -dependence only present in real corrections ($g(k_1) + g(k_2) \rightarrow \eta_Q(P) + g(k_3)$)



- Real-emission corrections are perfect square ($|\mathcal{M}^{(\text{Real})}|^2$) and thus positive
- IR singularities in the real emissions only reveal themselves after taking the

phase-space integration: $\bar{\sigma}_{gg}^{\text{NLO}, z \neq 1}(z) = \int d\hat{t} \frac{\bar{\sigma}_{gg}^{\text{NLO}, z \neq 1}}{d\hat{t}}$

$$\bar{\sigma}_{gg}^{\text{NLO}, z \neq 1}(z) = -\frac{1}{\epsilon_{\text{IR}}} \frac{\alpha_s}{\pi} \left(\frac{4\pi\mu_R^2}{M_Q^2} \right)^\epsilon \Gamma(1+\epsilon) \hat{\sigma}_0^{\text{LO}} z P_{gg}(z) + 2C_A \frac{\alpha_s}{\pi} \hat{\sigma}_0^{\text{LO}} \bar{A}_{gg}(z)$$

- For $\epsilon_{\text{IR}} \rightarrow 0^-$, $\bar{\sigma}_{gg}^{\text{NLO}, z \neq 1} \geq 0$ for all $0 \leq z < 1$ as expected
- Initial-state collinear divergences are absorbed/subtracted into PDF via *process-independent* Altarelli-Parisi counterterm in $\overline{\text{MS}}$ -scheme

$$\bar{\sigma}_{gg}^{\text{AP-CT}}(z) = \frac{1}{\epsilon_{\text{IR}}} \frac{\alpha_s}{\pi} \left(\frac{4\pi\mu_R^2}{\mu_F^2} \right)^\epsilon \Gamma(1+\epsilon) \hat{\sigma}_0^{\text{LO}} z P_{gg}(z)$$

A new scale-choice prescription

JPL, M.A. Ozcelik, EPJC 81 (2021) 6, 497

A new scale-choice prescription

JPL, M.A. Ozcelik, EPJC 81 (2021) 6, 497

- The subtraction of the AP CT in the $\overline{\text{MS}}$ -scheme then yields :

$$\lim_{z \rightarrow 0} \hat{\sigma}_{(g,q)g}^{\text{NLO}}(z) = (2C_A, C_F) \frac{\alpha_s}{\pi} \hat{\sigma}_0^{\text{LO}} \left(\log \frac{M_Q^2}{\mu_F^2} + A_{(g,q)g} \right) \quad (3)$$

A new scale-choice prescription

JPL, M.A. Ozcelik, EPJC 81 (2021) 6, 497

- The subtraction of the AP CT in the $\overline{\text{MS}}$ -scheme then yields :

$$\lim_{z \rightarrow 0} \hat{\sigma}_{(g,q)g}^{\text{NLO}}(z) = (2C_A, C_F) \frac{\alpha_s}{\pi} \hat{\sigma}_0^{\text{LO}} \left(\log \frac{M_Q^2}{\mu_F^2} + A_{(g,q)g} \right) \quad (3)$$

- In principle, the subtraction should be compensated by the PDF evolution

A new scale-choice prescription

JPL, M.A. Ozcelik, EPJC 81 (2021) 6, 497

- The subtraction of the AP CT in the $\overline{\text{MS}}$ -scheme then yields :

$$\lim_{z \rightarrow 0} \hat{\sigma}_{(g,q)g}^{\text{NLO}}(z) = (2C_A, C_F) \frac{\alpha_s}{\pi} \hat{\sigma}_0^{\text{LO}} \left(\log \frac{M_Q^2}{\mu_F^2} + A_{(g,q)g} \right) \quad (3)$$

- In principle, the subtraction should be compensated by the PDF evolution
- PDF evolution is universal, not $A_{ij} \rightarrow \hat{\sigma} < 0$ can arise from this subtraction

A new scale-choice prescription

JPL, M.A. Ozcelik, EPJC 81 (2021) 6, 497

- The subtraction of the AP CT in the $\overline{\text{MS}}$ -scheme then yields :

$$\lim_{z \rightarrow 0} \hat{\sigma}_{(g,q)g}^{\text{NLO}}(z) = (2C_A, C_F) \frac{\alpha_s}{\pi} \hat{\sigma}_0^{\text{LO}} \left(\log \frac{M_Q^2}{\mu_F^2} + A_{(g,q)g} \right) \quad (3)$$

- In principle, the subtraction should be compensated by the PDF evolution
- PDF evolution is universal, not $A_{ij} \rightarrow \hat{\sigma} < 0$ can arise from this subtraction
- $A_{gg} = A_{qg}$ allows us to propose a new scale prescription for μ_F ,

$$\boxed{\mu_F = \hat{\mu}_F \equiv M_Q e^{A_{gg,qg}/2}} \text{ such that } \left(\log \frac{M_Q^2}{\mu_F^2} + A_{gg,qg} \right) = 0 \text{ and } \lim_{z \rightarrow 0} \hat{\sigma}_{gg,qg}^{\text{NLO}}(z) = 0$$

A new scale-choice prescription

JPL, M.A. Ozcelik, EPJC 81 (2021) 6, 497

- The subtraction of the AP CT in the $\overline{\text{MS}}$ -scheme then yields :

$$\lim_{z \rightarrow 0} \hat{\sigma}_{(g,q)g}^{\text{NLO}}(z) = (2C_A, C_F) \frac{\alpha_s}{\pi} \hat{\sigma}_0^{\text{LO}} \left(\log \frac{M_Q^2}{\mu_F^2} + A_{(g,q)g} \right) \quad (3)$$

- In principle, the subtraction should be compensated by the PDF evolution
- PDF evolution is universal, not $A_{ij} \rightarrow \hat{\sigma} < 0$ can arise from this subtraction
- $A_{gg} = A_{qg}$ allows us to propose a new scale prescription for μ_F ,

$$\mu_F = \hat{\mu}_F \equiv M_Q e^{A_{gg,qg}/2} \text{ such that } \left(\log \frac{M_Q^2}{\mu_F^2} + A_{gg,qg} \right) = 0 \text{ and } \lim_{z \rightarrow 0} \hat{\sigma}_{gg,qg}^{\text{NLO}}(z) = 0$$

- All QCD radiations in the PDF evolution at $\hat{s} \rightarrow \infty$.
- $\hat{\mu}_F$ happens to be a point of minimal scale sensitivity at large \hat{s}

[Thanks to M. Nefedov for this observation]

A new scale-choice prescription

JPL, M.A. Ozcelik, EPJC 81 (2021) 6, 497

- The subtraction of the AP CT in the $\overline{\text{MS}}$ -scheme then yields :

$$\lim_{z \rightarrow 0} \hat{\sigma}_{(g,q)g}^{\text{NLO}}(z) = (2C_A, C_F) \frac{\alpha_s}{\pi} \hat{\sigma}_0^{\text{LO}} \left(\log \frac{M_Q^2}{\mu_F^2} + A_{(g,q)g} \right) \quad (3)$$

- In principle, the subtraction should be compensated by the PDF evolution
- PDF evolution is universal, not $A_{ij} \rightarrow \hat{\sigma} < 0$ can arise from this subtraction
- $A_{gg} = A_{qg}$ allows us to propose a new scale prescription for μ_F ,

$$\mu_F = \hat{\mu}_F \equiv M_Q e^{A_{gg,qg}/2} \text{ such that } \left(\log \frac{M_Q^2}{\mu_F^2} + A_{gg,qg} \right) = 0 \text{ and } \lim_{z \rightarrow 0} \hat{\sigma}_{gg,qg}^{\text{NLO}}(z) = 0$$

- All QCD radiations in the PDF evolution at $\hat{s} \rightarrow \infty$.
- $\hat{\mu}_F$ happens to be a point of minimal scale sensitivity at large \hat{s}

[Thanks to M. Nefedov for this observation]

- for η_Q we have $\hat{\mu}_F = \frac{M_Q}{\sqrt{e}} = \begin{cases} 1.82 \text{ GeV} & \text{for } \eta_c \text{ with } M_Q = 3 \text{ GeV} \\ 5.76 \text{ GeV} & \text{for } \eta_b \text{ with } M_Q = 9.5 \text{ GeV} \end{cases}$

A new scale-choice prescription

JPL, M.A. Ozcelik, EPJC 81 (2021) 6, 497

- The subtraction of the AP CT in the $\overline{\text{MS}}$ -scheme then yields :

$$\lim_{z \rightarrow 0} \hat{\sigma}_{(g,q)g}^{\text{NLO}}(z) = (2C_A, C_F) \frac{\alpha_s}{\pi} \hat{\sigma}_0^{\text{LO}} \left(\log \frac{M_Q^2}{\mu_F^2} + A_{(g,q)g} \right) \quad (3)$$

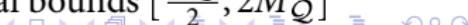
- In principle, the subtraction should be compensated by the PDF evolution
- PDF evolution is universal, not $A_{ij} \rightarrow \hat{\sigma} < 0$ can arise from this subtraction
- $A_{gg} = A_{qg}$ allows us to propose a new scale prescription for μ_F ,

$\mu_F = \hat{\mu}_F \equiv M_Q e^{A_{gg,qg}/2}$ such that $\left(\log \frac{M_Q^2}{\mu_F^2} + A_{gg,qg} \right) = 0$ and $\lim_{z \rightarrow 0} \hat{\sigma}_{gg,qg}^{\text{NLO}}(z) = 0$

- All QCD radiations in the PDF evolution at $\hat{s} \rightarrow \infty$.
- $\hat{\mu}_F$ happens to be a point of minimal scale sensitivity at large \hat{s}

[Thanks to M. Nefedov for this observation]

- for η_Q we have $\hat{\mu}_F = \frac{M_Q}{\sqrt{e}} = \begin{cases} 1.82 \text{GeV} & \text{for } \eta_c \text{ with } M_Q = 3 \text{GeV} \\ 5.76 \text{GeV} & \text{for } \eta_b \text{ with } M_Q = 9.5 \text{GeV} \end{cases}$
- Such scale choices for η_Q are within usual/conventional bounds $[\frac{M_Q}{2}, 2M_Q]$

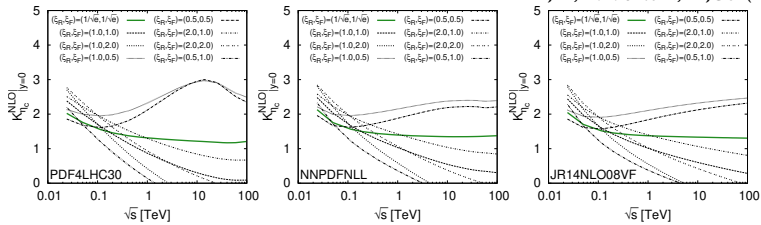


Our results with the $\hat{\mu}_F$ prescription

JPL, M.A. Ozcelik, EPJC 81 (2021) 6, 497

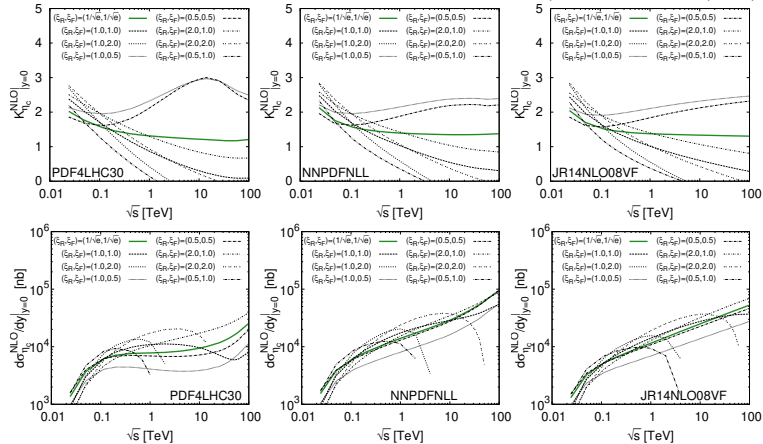
Our results with the $\hat{\mu}_F$ prescription

JPL, M.A. Ozcelik, EPJC 81 (2021) 6, 497



Our results with the $\hat{\mu}_F$ prescription

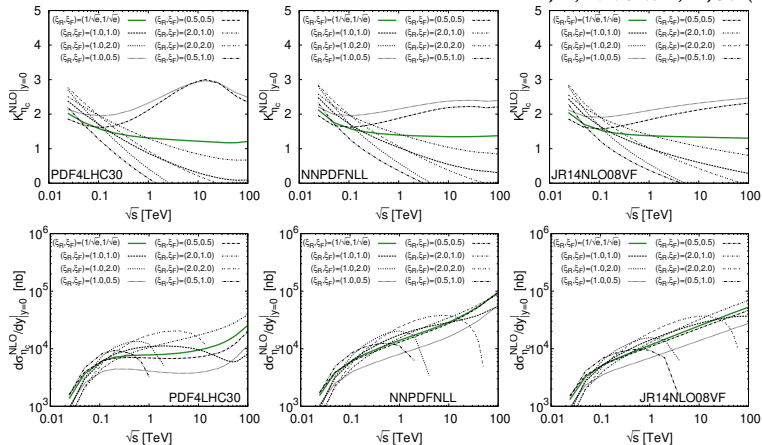
JPL, M.A. Ozcelik, EPJC 81 (2021) 6, 497



Problem solved, but it uncovers another: conventional NLO gluon PDFs exhibit a local minimum around $x = 0.001$ at scales below 2 GeV, which distorts $d\sigma(s)/dy$

Our results with the $\hat{\mu}_F$ prescription

JPL, M.A. Ozcelik, EPJC 81 (2021) 6, 497

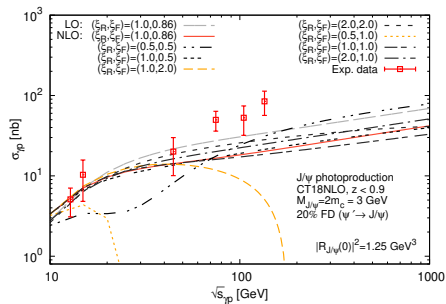


Problem solved, but it uncovers another: conventional NLO gluon PDFs exhibit a local minimum around $x = 0.001$ at scales below 2 GeV, which distorts $d\sigma(s)/dy$

Measuring η_c total cross sections (at NICA, LHC-FT and LHC) : crucial constraints on gluon PDFs

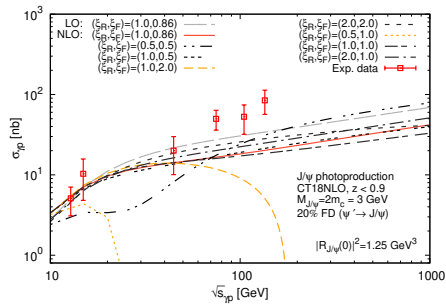
Same issue in J/ψ photoproduction

A. Colpani Serri, Y. Feng, C. Flore, J.P. Lansberg, M.A. Ozcelik, H.S. Shao, Y. Yedelkina: arXiv:2112.05060 [hep-ph]



Same issue in J/ψ photoproduction

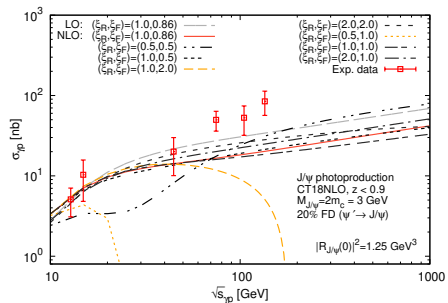
A. Colpani Serri, Y. Feng, C. Flore, J.P. Lansberg, M.A. Ozcelik, H.S. Shao, Y. Yedelkina: arXiv:2112.05060 [hep-ph]



- NLO cross section for J/ψ photoproduction becomes negative for large μ_F when $\sqrt{s_{J/\psi p}}$ increases

Same issue in J/ψ photoproduction

A. Colpani Serri, Y. Feng, C. Flore, J.P. Lansberg, M.A. Ozcelik, H.S. Shao, Y. Yedelkina: arXiv:2112.05060 [hep-ph]

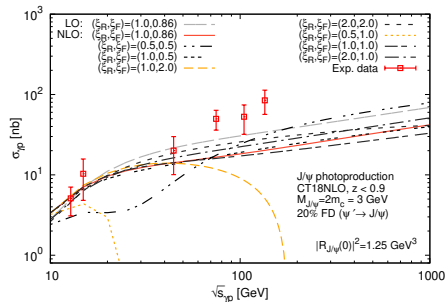


- NLO cross section for J/ψ photoproduction becomes negative for large μ_F when $\sqrt{s_{J/\psi p}}$ increases
- For $\mu_F = M_Q$, $\sigma < 0$ like for η_c hadroproduction

J.P. Lansberg, M.A. Ozcelik: Eur.Phys.J.C 81 (2021) 6, 497

Same issue in J/ψ photoproduction

A. Colpani Serri, Y. Feng, C. Flore, J.P. Lansberg, M.A. Ozcelik, H.S. Shao, Y. Yedelkina: arXiv:2112.05060 [hep-ph]



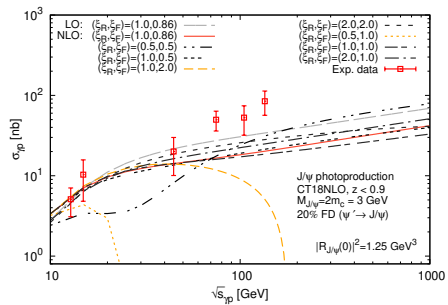
- NLO cross section for J/ψ photoproduction becomes negative for large μ_F when $\sqrt{s_{J/\psi p}}$ increases
- For $\mu_F = M_Q$, $\sigma < 0$ like for η_c hadroproduction

J.P. Lansberg, M.A. Ozcelik: Eur.Phys.J.C 81 (2021) 6, 497

- 2 possible sources of negative partonic cross sections: loop corrections (interference) and from real emission (subtraction of IR poles)

Negative cross-section values

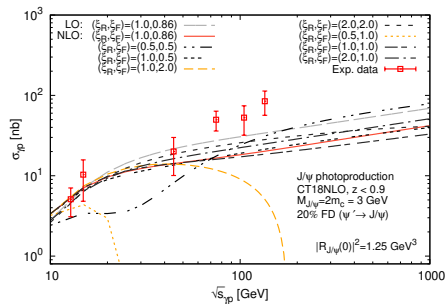
A. Colpani Serri, Y. Feng, C. Flore, J.P. Lansberg, M.A. Ozcelik, H.S. Shao, Y. Yedelkina: arXiv:2112.05060 [hep-ph]



- Initial state collinear divergences are removed via the subtraction into the PDFs via AP-CT

Negative cross-section values

A. Colpani Serri, Y. Feng, C. Flore, J.P. Lansberg, M.A. Ozcelik, H.S. Shao, Y. Yedelkina: arXiv:2112.05060 [hep-ph]



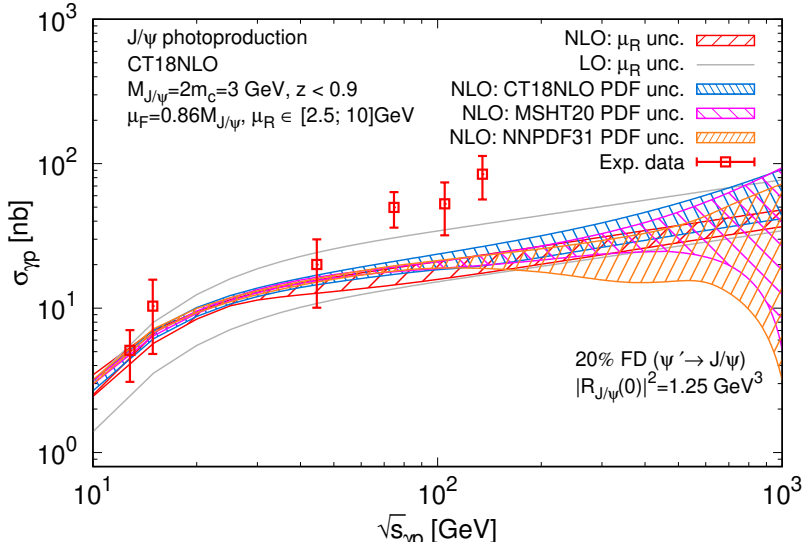
- Initial state collinear divergences are removed via the subtraction into the PDFs via AP-CT

- $\hat{s} \rightarrow \infty : \hat{\sigma}_{\gamma i}^{NLO} \propto \alpha_s(\mu_R) \left(\bar{c}_1^{(\gamma i)} \log \frac{M_Q^2}{\mu_F^2} + c_1^{(\gamma i)} \right), A_{\gamma i} = \frac{c_1^{(\gamma i)}}{\bar{c}_1^{(\gamma i)}},$

$$A_{\gamma g} = A_{\gamma q}$$

Results with $\hat{\mu}_F = 0.86M_Q$

A. Colpani Serri, Y. Feng, C. Flore, J.P. Lansberg, M.A. Ozcelik, H.S. Shao, Y. Yedelkina: arXiv:2112.05060 [hep-ph]



High-Energy Factorisation (HEF) and the leading-log approximation

The leading-log approximation (LLA): $\sum_n \alpha_s^n \ln^{n-1} \left(\frac{\hat{s}}{M_Q^2} \right)$ [Collins, Ellis, 91'; Catani, Ciafaloni, Hautmann, 91', 94']

High-Energy Factorisation (HEF) and the leading-log approximation

The leading-log approximation (LLA): $\sum_n \alpha_s^n \ln^{n-1} \left(\frac{\hat{s}}{M_Q^2} \right)$ [Collins, Ellis, 91'; Catani, Ciafaloni, Hautmann, 91', 94']

Defining $z = \frac{M_Q^2}{\hat{s}}$, one can face large $\ln 1/z$ when s becomes large

High-Energy Factorisation (HEF) and the leading-log approximation

The leading-log approximation (LLA): $\sum_n \alpha_s^n \ln^{n-1} \left(\frac{\hat{s}}{M_Q^2} \right)$ [Collins, Ellis, 91'; Catani, Ciafaloni, Hautmann, 91', 94']

Defining $z = \frac{M_Q^2}{\hat{s}}$, one can face **large $\ln 1/z$** when s becomes large

The **resummation** of such logs can be done through HEF.

High-Energy Factorisation (HEF) and the leading-log approximation

The leading-log approximation (LLA): $\sum_n \alpha_s^n \ln^{n-1} \left(\frac{\hat{s}}{M_Q^2} \right)$ [Collins, Ellis, 91'; Catani, Ciafaloni, Hautmann, 91', 94']

Defining $z = \frac{M_Q^2}{\hat{s}}$, one can face large $\ln 1/z$ when s becomes large

The resummation of such logs can be done through HEF.

For quarkonium production through $2 \rightarrow 1$ processes at Born order, one has

$$\begin{aligned}\hat{\sigma}_{ij}^{[m], \text{HEF}}(z, \mu_F, \mu_R) &= \int_{-\infty}^{\infty} d\eta_Q \int_0^{\infty} d\mathbf{q}_{T1}^2 d\mathbf{q}_{T2}^2 \mathcal{C}_{gi} \left(\frac{M_T}{M} \sqrt{z} e^{\eta_Q}, \mathbf{q}_{T1}^2, \mu_F, \mu_R \right) \\ &\times \mathcal{C}_{gj} \left(\frac{M_T}{M} \sqrt{z} e^{-\eta_Q}, \mathbf{q}_{T2}^2, \mu_F, \mu_R \right) \mathcal{H}^{[m]}(\mathbf{q}_{T1}^2, \mathbf{q}_{T2}^2) + \text{NLL} + \mathcal{O}(z),\end{aligned}$$

High-Energy Factorisation (HEF) and the leading-log approximation

The leading-log approximation (LLA): $\sum_n \alpha_s^n \ln^{n-1} \left(\frac{\hat{s}}{M_Q^2} \right)$ [Collins, Ellis, 91'; Catani, Ciafaloni, Hautmann, 91'94']

Defining $z = \frac{M_Q^2}{\hat{s}}$, one can face large $\ln 1/z$ when s becomes large

The resummation of such logs can be done through HEF.

For quarkonium production through $2 \rightarrow 1$ processes at Born order, one has

$$\hat{\sigma}_{ij}^{[m], \text{HEF}}(z, \mu_F, \mu_R) = \int_{-\infty}^{\infty} d\eta_Q \int_0^{\infty} d\mathbf{q}_{T1}^2 d\mathbf{q}_{T2}^2 \mathcal{C}_{gi} \left(\frac{M_T}{M} \sqrt{z} e^{\eta_Q}, \mathbf{q}_{T1}^2, \mu_F, \mu_R \right) \\ \times \mathcal{C}_{gj} \left(\frac{M_T}{M} \sqrt{z} e^{-\eta_Q}, \mathbf{q}_{T2}^2, \mu_F, \mu_R \right) \mathcal{H}^{[m]}(\mathbf{q}_{T1}^2, \mathbf{q}_{T2}^2) + \text{NLL} + \mathcal{O}(z),$$

$\mathcal{H}^{[m]}$ known at LO in α_s [Hagler et.al, 2000; Kniehl, Vasin, Saleev 2006] for $m = {}^1S_0^{(1,8)}, {}^3P_J^{(1,8)}, {}^3S_1^{(8)}$.
These are tree-level “squared matrix elements” of the $2 \rightarrow 1$ -type process:

$$R_+(\mathbf{q}_{T1}, q_1^+) + R_-(\mathbf{q}_{T2}, q_2^-) \rightarrow Q\bar{Q}[m].$$

High-Energy Factorisation (HEF) and the leading-log approximation

The leading-log approximation (LLA): $\sum_n \alpha_s^n \ln^{n-1} \left(\frac{\hat{s}}{M_Q^2} \right)$ [Collins, Ellis, 91'; Catani, Ciafaloni, Hautmann, 91'94']

Defining $z = \frac{M_Q^2}{\hat{s}}$, one can face large $\ln 1/z$ when s becomes large

The resummation of such logs can be done through HEF.

For quarkonium production through $2 \rightarrow 1$ processes at Born order, one has

$$\begin{aligned}\hat{\sigma}_{ij}^{[m], \text{HEF}}(z, \mu_F, \mu_R) &= \int_{-\infty}^{\infty} d\eta_Q \int_0^{\infty} d\mathbf{q}_{T1}^2 d\mathbf{q}_{T2}^2 \mathcal{C}_{gi} \left(\frac{M_T}{M} \sqrt{z} e^{\eta_Q}, \mathbf{q}_{T1}^2, \mu_F, \mu_R \right) \\ &\times \mathcal{C}_{gj} \left(\frac{M_T}{M} \sqrt{z} e^{-\eta_Q}, \mathbf{q}_{T2}^2, \mu_F, \mu_R \right) \mathcal{H}^{[m]}(\mathbf{q}_{T1}^2, \mathbf{q}_{T2}^2) + \text{NLL} + \mathcal{O}(z),\end{aligned}$$

$\mathcal{H}^{[m]}$ known at LO in α_s [Hagler *et.al.*, 2000; Kniehl, Vasin, Saleev 2006] for $m = {}^1S_0^{(1,8)}, {}^3P_J^{(1,8)}, {}^3S_1^{(8)}$.
These are tree-level “squared matrix elements” of the $2 \rightarrow 1$ -type process:

$$R_+(\mathbf{q}_{T1}, q_1^+) + R_-(\mathbf{q}_{T2}, q_2^-) \rightarrow Q\bar{Q}[m].$$

The resummation factors \mathcal{C} are the solution of the LL **BFKL** equation
with the collinear divergences subtracted

High-Energy Factorisation (HEF) and the leading-log approximation

The leading-log approximation (LLA): $\sum_n \alpha_s^n \ln^{n-1} \left(\frac{\hat{s}}{M_Q^2} \right)$ [Collins, Ellis, 91'; Catani, Ciafaloni, Hautmann, 91'94']

Defining $z = \frac{M_Q^2}{\hat{s}}$, one can face large $\ln 1/z$ when s becomes large

The resummation of such logs can be done through HEF.

For quarkonium production through $2 \rightarrow 1$ processes at Born order, one has

$$\begin{aligned}\hat{\sigma}_{ij}^{[m], \text{HEF}}(z, \mu_F, \mu_R) &= \int_{-\infty}^{\infty} d\eta_Q \int_0^{\infty} d\mathbf{q}_{T1}^2 d\mathbf{q}_{T2}^2 \mathcal{C}_{gi} \left(\frac{M_T}{M} \sqrt{z} e^{\eta_Q}, \mathbf{q}_{T1}^2, \mu_F, \mu_R \right) \\ &\times \mathcal{C}_{gj} \left(\frac{M_T}{M} \sqrt{z} e^{-\eta_Q}, \mathbf{q}_{T2}^2, \mu_F, \mu_R \right) \mathcal{H}^{[m]}(\mathbf{q}_{T1}^2, \mathbf{q}_{T2}^2) + \text{NLL} + \mathcal{O}(z),\end{aligned}$$

$\mathcal{H}^{[m]}$ known at LO in α_s [Hagler *et.al.*, 2000; Kniehl, Vasin, Saleev 2006] for $m = {}^1S_0^{(1,8)}, {}^3P_J^{(1,8)}, {}^3S_1^{(8)}$.
These are tree-level “squared matrix elements” of the $2 \rightarrow 1$ -type process:

$$R_+(\mathbf{q}_{T1}, q_1^+) + R_-(\mathbf{q}_{T2}, q_2^-) \rightarrow Q\bar{Q}[m].$$

The resummation factors \mathcal{C} are the solution of the LL **BFKL** equation
with the collinear divergences subtracted
 $\mathcal{O}(z)$ terms (without $\ln 1/z$) cannot be captured by HEF (see later)

High-energy factorisation for photoproduction

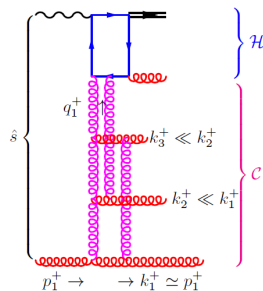
$$\hat{\sigma}_{\text{HEF}}(\eta) \propto \int_0^{1+\eta} \frac{dy}{y} \int_0^{\infty} d\mathbf{q}_{T1}^2 \mathcal{C}\left(\frac{y}{1+\eta}, \mathbf{q}_{T1}^2, \mu_F, \mu_R\right) \mathcal{H}(y, \mathbf{q}_{T1}^2) + \text{NLLA} + O(1/\eta)$$

High-energy factorisation for photoproduction

$$\hat{\sigma}_{\text{HEF}}(\eta) \propto \int_0^{1+\eta} \frac{dy}{y} \int_0^\infty d\mathbf{q}_{T1}^2 \mathcal{C}\left(\frac{y}{1+\eta}, \mathbf{q}_{T1}^2, \mu_F, \mu_R\right) \mathcal{H}(y, \mathbf{q}_{T1}^2) + \text{NLLA} + O(1/\eta)$$

Physical picture in the **LLA**
for photoproduction:

- Here one resums $\sum_n \alpha_s^n \ln^{n-1}(1+\eta)$ [$\eta = (\hat{s} - M_Q^2)/M_Q^2$]



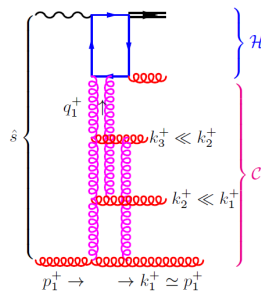
Glauber exchanges ($k_+ k_- \ll \mathbf{k}_T^2$) form the

Reggeised gluon in the t -channel.

High-energy factorisation for photoproduction

$$\hat{\sigma}_{\text{HEF}}(\eta) \propto \int_0^{1+\eta} \frac{dy}{y} \int_0^\infty d\mathbf{q}_{T1}^2 \mathcal{C}\left(\frac{y}{1+\eta}, \mathbf{q}_{T1}^2, \mu_F, \mu_R\right) \mathcal{H}(y, \mathbf{q}_{T1}^2) + \text{NLLA} + O(1/\eta)$$

Physical picture in the **LLA** for photoproduction:



- Here one resums $\sum_n \alpha_s^n \ln^{n-1}(1+\eta)$ [$\eta = (\hat{s} - M_Q^2)/M_Q^2$]

- For consistency with fixed-order **DGLAP** evolution the anomalous dimension γ_{gg} in \mathcal{C} should be truncated:

$$\gamma_{gg}(N, \alpha_s) = \underbrace{\frac{\hat{\alpha}_s}{N} + 2\zeta(3)\frac{\hat{\alpha}_s^4}{N^4} + 2\zeta(5)\frac{\hat{\alpha}_s^6}{N^6} + \dots}_{\text{DLA}} \underbrace{\quad\quad\quad}_{\text{LLA}}$$

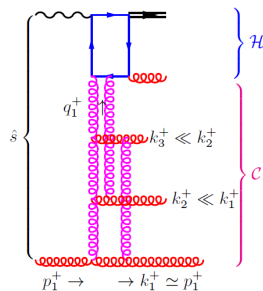
Glauber exchanges ($k_+ k_- \ll \mathbf{k}_T^2$) form the

Reggeised gluon in the t -channel.

High-energy factorisation for photoproduction

$$\hat{\sigma}_{\text{HEF}}(\eta) \propto \int_0^{1+\eta} \frac{dy}{y} \int_0^\infty d\mathbf{q}_{T1}^2 \mathcal{C}\left(\frac{y}{1+\eta}, \mathbf{q}_{T1}^2, \mu_F, \mu_R\right) \mathcal{H}(y, \mathbf{q}_{T1}^2) + \text{NLLA} + O(1/\eta)$$

Physical picture in the **LLA** for photoproduction:



- Here one resums $\sum_n \alpha_s^n \ln^{n-1}(1+\eta)$ [$\eta = (\hat{s} - M_Q^2)/M_Q^2$]

- For consistency with fixed-order **DGLAP** evolution the anomalous dimension γ_{gg} in \mathcal{C} should be truncated:

$$\gamma_{gg}(N, \alpha_s) = \underbrace{\frac{\hat{\alpha}_s}{N}}_{\text{DLA}} + 2\zeta(3) \frac{\hat{\alpha}_s^4}{N^4} + 2\zeta(5) \frac{\hat{\alpha}_s^6}{N^6} + \dots$$

$\overbrace{\hspace{10em}}$ LLA

- Expansion of $\hat{\sigma}_{\text{HEF}}(\eta)$ in α_s **correctly reproduces** $\hat{\sigma}_{\text{NLO}}(\eta \gg 1)$ and predicts the $\hat{\sigma}_{\text{NNLO}}(\eta \gg 1)$

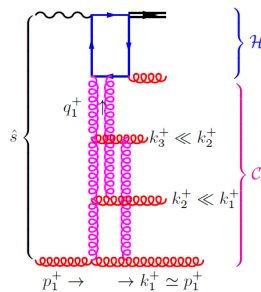
Glauber exchanges ($k_+ k_- \ll \mathbf{k}_T^2$) form the

Reggeised gluon in the t -channel.

High-energy factorisation for photoproduction

$$\hat{\sigma}_{\text{HEF}}(\eta) \propto \int_0^{1+\eta} \frac{dy}{y} \int_0^\infty d\mathbf{q}_{T1}^2 \mathcal{C}\left(\frac{y}{1+\eta}, \mathbf{q}_{T1}^2, \mu_F, \mu_R\right) \mathcal{H}(y, \mathbf{q}_{T1}^2) + \text{NLLA} + O(1/\eta)$$

Physical picture in the **LLA** for photoproduction:



Glauber exchanges ($k_+ k_- \ll \mathbf{k}_T^2$) form the

Reggeised gluon in the t -channel.

- Here one resums $\sum_n \alpha_s^n \ln^{n-1}(1+\eta)$ [$\eta = (\hat{s} - M_Q^2)/M_Q^2$]

- For consistency with fixed-order **DGLAP** evolution the anomalous dimension γ_{gg} in \mathcal{C} should be truncated:

$$\gamma_{gg}(N, \alpha_s) = \underbrace{\frac{\hat{\alpha}_s}{N}}_{\text{DLA}} + 2\zeta(3) \frac{\hat{\alpha}_s^4}{N^4} + 2\zeta(5) \frac{\hat{\alpha}_s^6}{N^6} + \dots$$

$\overbrace{\hspace{10em}}$
LLA

- Expansion of $\hat{\sigma}_{\text{HEF}}(\eta)$ in α_s **correctly reproduces** $\hat{\sigma}_{\text{NLO}}(\eta \gg 1)$ and predicts the $\hat{\sigma}_{\text{NNLO}}(\eta \gg 1)$
- Note: the coefficient function \mathcal{H} should be calculated at NLO for **NLLA**,

Consistency check

J.P. Lansberg, M. Nefedov, M.A.Ozcelik, JHEP 05 (2022) 083

HEF expanded up to NLO in α_s should reproduce the $A_1^{[m]}$ NLO coefficient

Consistency check

J.P. Lansberg, M. Nefedov, M.A.Ozcelik, JHEP 05 (2022) 083

HEF expanded up to NLO in α_s should reproduce the $A_1^{[m]}$ NLO coefficient
High-energy limit (for η_Q):

$$\begin{aligned}\hat{\sigma}_{gg}^{[m], \text{HEF}}(z \rightarrow 0) = & \sigma_{\text{LO}}^{[m]} \left\{ A_0^{[m]} \delta(1-z) + \frac{\alpha_s}{\pi} 2C_A \left[A_1^{[m]} + A_0^{[m]} \ln \frac{M^2}{\mu_F^2} \right] \right. \\ & \left. + \left(\frac{\alpha_s}{\pi} \right)^2 \ln \frac{1}{z} C_A^2 \left[2A_2^{[m]} + B_2^{[m]} + 4A_1^{[m]} \ln \frac{M^2}{\mu_F^2} + 2A_0^{[m]} \ln^2 \frac{M^2}{\mu_F^2} \right] + O(\alpha_s^3) \right\},\end{aligned}$$

Consistency check

J.P. Lansberg, M. Nefedov, M.A.Ozcelik, JHEP 05 (2022) 083

HEF expanded up to NLO in α_s should reproduce the $A_1^{[m]}$ NLO coefficient
High-energy limit (for η_Q):

$$\hat{\sigma}_{gg}^{[m], \text{HEF}}(z \rightarrow 0) = \sigma_{\text{LO}}^{[m]} \left\{ A_0^{[m]} \delta(1-z) + \frac{\alpha_s}{\pi} 2C_A \left[A_1^{[m]} + A_0^{[m]} \ln \frac{M^2}{\mu_F^2} \right] + \left(\frac{\alpha_s}{\pi} \right)^2 \ln \frac{1}{z} C_A^2 \left[2A_2^{[m]} + B_2^{[m]} + 4A_1^{[m]} \ln \frac{M^2}{\mu_F^2} + 2A_0^{[m]} \ln^2 \frac{M^2}{\mu_F^2} \right] + O(\alpha_s^3) \right\},$$

From HEF, up to NNLO, one has

State	$A_0^{[m]}$	$A_1^{[m]}$	$A_2^{[m]}$	$B_2^{[m]}$
1S_0	1	-1	$\frac{\pi^2}{6}$	$\frac{\pi^2}{6}$
3S_1	0	1	0	$\frac{\pi^2}{6}$
3P_0	1	$-\frac{43}{27}$	$\frac{\pi^2}{6} + \frac{2}{3}$	$\frac{\pi^2}{6} + \frac{40}{27}$
3P_1	0	$\frac{5}{54}$	$-\frac{1}{9}$	$-\frac{2}{9}$
3P_2	1	$-\frac{53}{36}$	$\frac{\pi^2}{6} + \frac{1}{2}$	$\frac{\pi^2}{6} + \frac{11}{9}$

Consistency check

J.P. Lansberg, M. Nefedov, M.A. Ozcelik, JHEP 05 (2022) 083

HEF expanded up to NLO in α_s should reproduce the $A_1^{[m]}$ NLO coefficient
 High-energy limit (for η_Q):

$$\hat{\sigma}_{gg}^{[m], \text{HEF}}(z \rightarrow 0) = \sigma_{\text{LO}}^{[m]} \left\{ A_0^{[m]} \delta(1-z) + \frac{\alpha_s}{\pi} 2C_A \left[A_1^{[m]} + A_0^{[m]} \ln \frac{M^2}{\mu_F^2} \right] + \left(\frac{\alpha_s}{\pi} \right)^2 \ln \frac{1}{z} C_A^2 \left[2A_2^{[m]} + B_2^{[m]} + 4A_1^{[m]} \ln \frac{M^2}{\mu_F^2} + 2A_0^{[m]} \ln^2 \frac{M^2}{\mu_F^2} \right] + O(\alpha_s^3) \right\},$$

From HEF, up to NNLO, one has

State	$A_0^{[m]}$	$A_1^{[m]}$	$A_2^{[m]}$	$B_2^{[m]}$
1S_0	1	-1	$\frac{\pi^2}{6}$	$\frac{\pi^2}{6}$
3S_1	0	1	0	$\frac{\pi^2}{6}$
3P_0	1	$-\frac{43}{27}$	$\frac{\pi^2}{6} + \frac{2}{3}$	$\frac{\pi^2}{6} + \frac{40}{27}$
3P_1	0	$\frac{5}{54}$	$-\frac{1}{9}$	$-\frac{2}{9}$
3P_2	1	$-\frac{53}{36}$	$\frac{\pi^2}{6} + \frac{1}{2}$	$\frac{\pi^2}{6} + \frac{11}{9}$

Perfect match for NLO and prediction for NNLO !

NLO: JPL, M.A. Ozcelik, EPJC 81 (2021) 6, 497

Matching HEF and NLO CF (illustration for η_Q)

The HEF works only at $z \ll 1$ and does not include corrections $O(z)$, while NLO CF is exact in z but only NLO up to α_s . **We need to match them.**

- Simplest prescription: just **subtract the overlap** at $z \ll 1$:

$$\sigma_{\text{NLO+HEF}}^{[m]} = \sigma_{\text{LO CF}}^{[m]} + \int_{z_{\min}}^1 \frac{dz}{z} \left[\check{\sigma}_{\text{HEF}}^{[m],ij}(z) + \hat{\sigma}_{\text{NLO CF}}^{[m],ij}(z) - \hat{\sigma}_{\text{NLO CF}}^{[m],ij}(0) \right] \mathcal{L}_{ij}(z)$$

- Or introduce **smooth weights**:

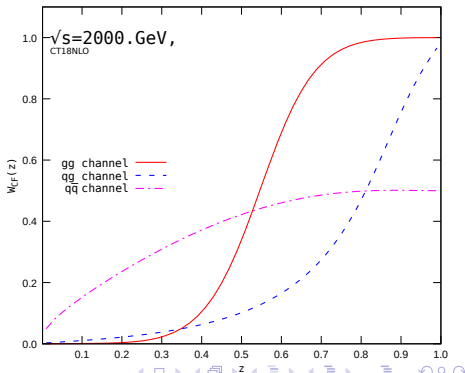
$$\begin{aligned} \sigma_{\text{NLO+HEF}}^{[m]} = & \sigma_{\text{LO CF}}^{[m]} + \int_{z_{\min}}^1 dz \left\{ \left[\check{\sigma}_{\text{HEF}}^{[m],ij}(z) \frac{\mathcal{L}_{ij}(z)}{z} \right] w_{\text{HEF}}^{ij}(z) \right. \\ & \left. + \left[\hat{\sigma}_{\text{NLO CF}}^{[m],ij}(z) \frac{\mathcal{L}_{ij}(z)}{z} \right] (1 - w_{\text{HEF}}^{ij}(z)) \right\}, \end{aligned}$$

Inverse error weighting method (illustration for η_Q)

In the InEW method [Echevarria, et.al., 2018] the weights are calculated from the **parametric estimates of the error** of each contribution and combined as such:

$$w_{\text{HEF}}^{ij}(z) = \frac{[\Delta\sigma_{\text{HEF}}^{ij}(z)]^{-2}}{[\Delta\sigma_{\text{HEF}}^{ij}(z)]^{-2} + [\Delta\sigma_{\text{CF}}^{ij}(z)]^{-2}},$$

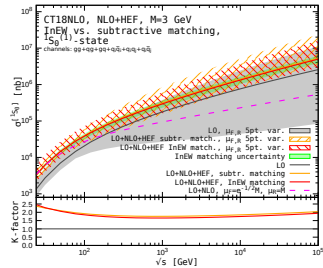
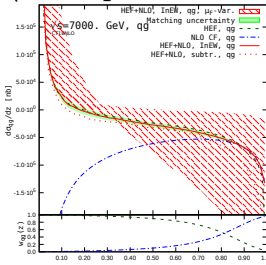
- For $\Delta\sigma_{\text{CF}}$, we take the NNLO $\alpha_s^2 \ln \frac{1}{z}$ term of $\hat{\sigma}(z)$ predicted by HEF,
- For $\Delta\sigma_{\text{HEF}}$, we take the $\alpha_s O(z)$ part of the NLO CF result for $\hat{\sigma}(z)$.
- In both cases, stability against $O(\alpha_s^2)$ (constant in z , unknown) corrections is checked



Matched results

η_c hadroproduction

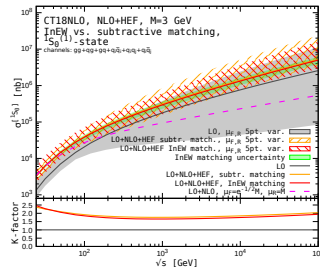
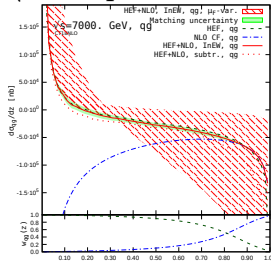
J.P. Lansberg, M. Nefedov, M.A.Ozcelik, JHEP 05 (2022) 083 and to appear



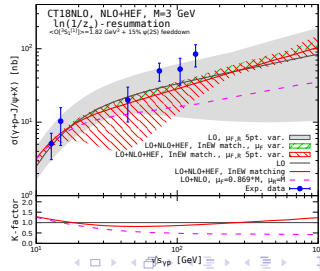
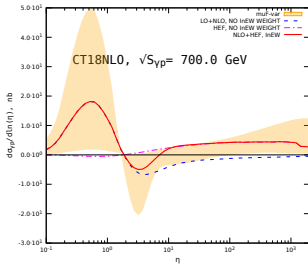
Matched results

η_c hadroproduction

J.P. Lansberg, M. Nefedov, M.A.Ozcelik, JHEP 05 (2022) 083 and to appear



J/ψ photoproduction



Summary

Summary

- Source of negative NLO cross sections in quarkonium production (NRQCD) identified and cured

Summary

- Source of **negative NLO cross sections** in quarkonium production (NRQCD) **identified** and **cured**
- $\hat{\mu}_F$ scale prescription introduced: sufficient if ones sticks to collinear factorisation at NLO

Summary

- Source of negative NLO cross sections in quarkonium production (NRQCD) identified and cured
- $\hat{\mu}_F$ scale prescription introduced: sufficient if ones sticks to collinear factorisation at NLO
- HEF provides a more complete solution beyond collinear factorisation but needs to be matched to it

Summary

- Source of negative NLO cross sections in quarkonium production (NRQCD) identified and cured
- $\hat{\mu}_F$ scale prescription introduced: sufficient if ones sticks to collinear factorisation at NLO
- HEF provides a more complete solution beyond collinear factorisation but needs to be matched to it
- Waiting now for η_Q hadroproduction data (FT-LHC) and J/ψ photoproduction data from EIC and inclusive UPC at LHC

Summary

- Source of **negative NLO cross sections** in quarkonium production (NRQCD) **identified** and **cured**
- $\hat{\mu}_F$ scale prescription introduced: sufficient if ones sticks to collinear factorisation at NLO
- HEF provides **a more complete solution** beyond collinear factorisation but needs to be matched to it
- Waiting now for η_Q hadroproduction data (FT-LHC) and J/ψ photoproduction data from EIC and **inclusive** UPC at LHC
- More to be learnt about this in the coming months:

Summary

- Source of negative NLO cross sections in quarkonium production (NRQCD) identified and cured
- $\hat{\mu}_F$ scale prescription introduced: sufficient if ones sticks to collinear factorisation at NLO
- HEF provides a more complete solution beyond collinear factorisation but needs to be matched to it
- Waiting now for η_Q hadroproduction data (FT-LHC) and J/ψ photoproduction data from EIC and inclusive UPC at LHC
- More to be learnt about this in the coming months:
 - QCD@LHC2022 in Orsay, Nov. 28 - Dec. 2, 2022

Summary

- Source of **negative NLO cross sections** in quarkonium production (NRQCD) **identified** and **cured**
- $\hat{\mu}_F$ scale prescription introduced: sufficient if ones sticks to collinear factorisation at NLO
- HEF provides **a more complete solution** beyond collinear factorisation but needs to be matched to it
- Waiting now for η_Q hadroproduction data (FT-LHC) and J/ψ photoproduction data from EIC and **inclusive** UPC at LHC
- More to be learnt about this in the coming months:
 - QCD@LHC2022 in Orsay, Nov. 28 - Dec. 2, 2022
 - Quarkonia as Tools 2023 in Aussois, Jan. 9 - 14, 2023

Summary

- Source of **negative NLO cross sections** in quarkonium production (NRQCD) **identified** and **cured**
- $\hat{\mu}_F$ scale prescription introduced: sufficient if ones sticks to collinear factorisation at NLO
- HEF provides **a more complete solution** beyond collinear factorisation but needs to be matched to it
- Waiting now for η_Q hadroproduction data (FT-LHC) and J/ψ photoproduction data from EIC and **inclusive** UPC at LHC
- More to be learnt about this in the coming months:
 - QCD@LHC2022 in Orsay, Nov. 28 - Dec. 2, 2022
 - Quarkonia as Tools 2023 in Aussois, Jan. 9 - 14, 2023
 - QCDEvolution 2023 in Orsay, May 22-26, 2023

A EU Virtual Access to pQCD tools: NLOAccess

[in2p3.fr/nloaccess]

NLOAccess

Virtual Access: Automated perturbative NLO calculations for heavy ions and quarkonia (NLOAccess)

Home The project ▾ News ▾ Tools ▾ Request registration

GENERAL DESCRIPTION

Objectives:

NLOAccess will give access to automated tools generating scientific codes allowing anyone to evaluate observables -such as production rates or kinematical properties – of scatterings involving hadrons. The automation and the versatility of these tools are such that these scatterings need not to be pre-coded. In other terms, it is possible that a random user may request for the first time the generation of a code to compute characteristics of a reaction which nobody thought of before. NLOAccess will allow the user to test the code and then to download to run it on its own computer. It essentially gives access to a dynamical library

[Show more](#)

FOLLOW:

STRONG 2020

This project has received funding from the European Union's Horizon 2020 research and innovation programme under grant agreement No. 824093.

HELAC-Onia Web [nloaccess.in2p3.fr/HO/]

HELAC-Onia Web

[Request Registration](#)

[References](#)

[Contact us](#)

[Login](#)



Automated perturbative calculation with HELAC-Onia Web

Welcome to HELAC-Onia Web!

HELAC-Onia is an automatic matrix element generator for the calculation of the heavy quarkonium helicity amplitudes in the framework of NRQCD factorization.

The program is able to calculate helicity amplitudes of multi P-wave quarkonium states production at hadron colliders and electron-positron colliders by including new P-wave off-shell currents. Besides the high efficiencies in computation of multi-leg processes within the Standard Model, HELAC-Onia is also sufficiently numerical stable in dealing with P-wave quarkonia and P-wave color-octet intermediate states.

Already registered to the portal? Please [login](#).

Do you not have an account? Make a [registration request](#).



MG5@NLO online [nloaccess.in2p3.fr/MG5/]

 MG5_aMC@NLO

[Request Registration](#)

[References](#)

 [Contact us](#)

 [Login](#)



Automated perturbative calculation with NLOAccess

MG5_aMC@NLO

MadGraph5_aMC@NLO is a framework that aims at providing all the elements necessary for SM and BSM phenomenology, such as the computations of cross sections, the generation of hard events and their matching with event generators, and the use of a variety of tools relevant to event manipulation and analysis. Processes can be simulated to LO accuracy for any user-defined Lagrangian, an the NLO accuracy in the case of models that support this kind of calculations -- prominent among these are QCD and EW corrections to SM processes. Matrix elements at the tree- and one-loop-level can also be obtained.

Please login to use MG5_aMC@NLO.

